Finite element method numerical simulation and ductile capacity analysis of bond-slip between epoxy coated plain steel bars and concrete

K. Kazakov[1] & A. Yanakieva[2]
[1]*Structural Mechanics Department, Higher School of Civil Engineering, Bulgaria*
[2]*Institute of Mechanics, Bulgarian Academy of Science, Bulgaria*

Abstract

This research is devoted to a finite element method (FEM) numerical simulation of the bond-slip between epoxy coated plain steel bars and concrete and the ductile capacity of the mechanical process of extracting the steel bars. In this case the cured epoxy coating is assumed to be mid-layer, located between the steel bar and the concrete. This layer leads to a change of the ductile capacity of the bond and to some differences in the nonlinear bond-slip relation in comparison with the bond-slip relation in the case of non-insulated steel bars. The aim of the research is the generation of an adequate numerical model for extracting the bond-slip relation. For that purpose, a more realistic concrete material model is assumed in the proposed computational model, by means of development of dispersion micro cracks. The pull-out force is compared with the force recorded in an experiment.

The ductile capacity of the bond is also analyzed and discussed in detail. The analysis is performed by the FEM.

Keywords: FEM contact problems, bond-slip relation, ductile capacity, epoxy coated plane steel bars.

1 Introduction

A good bond between the steel reinforcing bar and concrete in concrete structures is decisive for structural and durable performance. If this bond is

WIT Transactions on Engineering Sciences, Vol 62, © 2009 WIT Press
www.witpress.com, ISSN 1743-3533 (on-line)
doi:10.2495/SECM090201

inadequate, the behaviour and failure development can be altered. Very often in engineering practice, the steel used in the reinforced concrete elements is isolated by epoxy coating. Such a coating influences the bond-slip relation and pull-out force, i.e. the ultimate force, during the extraction process.

In the last three decades, many papers have been reported in this research area. In 1988 Gustafson [1] founds that coated deformable bars developed approximately 66% of the bond strength of the uncoated bars. The tests showed that the epoxy coating, whatever its thickness, is essentially the bond breaker of the adhesion bond. Choi *et al.* [2] consider the effect of various factors including coating thickness, bar size and deformation pattern. The effect of epoxy coating thickness on bond strength is also evaluated by Miller *et al.* [3]. In their experimental study, Cleary and Ramirez [4] compared the effect of repeated loading on the service behaviour and ultimate bond strength of reinforced concrete members containing epoxy-coated reinforcement to that of members with uncoated reinforcement. Kayyali and Yeomans [5] report the results of investigation into the bond of epoxy coated reinforcement in concrete beams acting in flexure, compared to that using pullout testing. Hamad [6] and Ldun and Darwin [7] assess the effect of rib geometry/rib angle, rib spacing, rib height and concrete strength on the relative bond-slip characteristics of coated and uncoated deformed bars. The value of bar-friction coefficient has been obtained (Prostatio [8]) by testing a concrete tension strut reinforced with a manually applied epoxy coated steel bar. In conclusion, there are many studies that take into account and discuss the parameters that influence bond behaviour, but these are mainly from test procedures [9, 10]. Besides, more of these investigations are assigned to deformable bars. The joineries in the precast concrete structures are prepared by plain steel bars welded to some built-in reinforcement. Placing the plain rebars along either side of the joint will strengthen its resistance and provide greater ductility. Therefore, the bond properties of plain bars in concrete need to be understood (Mo and Chan [11]).

In this paper two computational models are proposed. The results corresponding to the pull-out process bond-slip relations are excerpted and the ultimate extraction forces are obtained. The simulations are based on a step-by-step extraction of an isolated steel bar from a concrete body and strictly adhere to the experimental settings, reported in [12]. The first model, called Model A, is based on the précised multi-linear stress-strain concrete relation. This model is compared with a computational model, reported by the authors in [13]. In the second model, called Model B, in addition to Model A, the development of dispersion micro cracks is included.

The components, those that significantly influence the bond-slip behaviour, are discussed in detail. The so-called ductility capacity of the bond is also investigated.

2 Finite element method contact technology

Finite element method (FEM) contact technology requires a fine step-by-step increment to assure a smooth transfer of contact forces and iteration stability. If

the interaction area is a surface, the corresponding adequate computational model should be generated by surface-to-surface contact elements [14]. Such a model recognizes possible contact pairs by the presence of specific finite contact elements. These contact elements are overlaid on the part or parts of the model areas that are being analyzed for interaction.

2.1 Contact pair finite elements

The contact pairs contain two finite elements – contact and target elements with the same real constants as penetration, friction constant, maximum friction stress, contact surface offset, contact cohesion, tangent penalty stiffness factor, pinball region and etc.

Target elements are used to represent the body surface, in the present research it is the surface of the concrete block hole. In this paper, the so-called concrete solid finite element (CSFE) is used the concrete body to be discretized, see fig. 3. The solid is capable of cracking in tension and crushing in compression. The element is defined by four nodes and isotropic material properties. Target volume can be assumed as rigid or deformable. In the Model A and Model B, it is chosen as deformable, for the Poisson effect to be taken into account. Target elements are generated with an external surface that has the same shape and mesh as the underling solid elements. These elements have 4 nodes and 12 DOFs. Generally, in the FEM concept, target elements impose kinematic constrains which prevent penetration of one body through another. However, the computational models, discussed in the paper, are built in such a way that the contact of the steel surface and the concrete is taken as an initial. The contact can be closed only on some subareas of the contact zone due to the Poisson ratio. Some details, related to the theoretical aspects of the contact status, are discussed below.

Contact elements are used the steel bar surface to be discretized and to represent the contact and sliding between the 3D contact surfaces. Such an element overlies the solid elements describing the boundary of a deformable body, in the present research the steel bar, and is potentially in contact with the target surface. It has the same geometric characteristics as the solid with which it is connected. The rebar is discretized, see fig.3, by the so-called steel solid finite elements (SSFE).

Generally, contact occurs when the contact element surface penetrates one of the target segment elements on the specified target surface. In the present models, the contact and penetration are assumed as initial. The FEM module preliminary evaluates the model to detect the initial contact conditions. The target and contact elements are attached to the hollow radius of the concrete body and to the outer radius of the rebar, respectively. These elements are nonlinear and require a full Newton-Raphson iterative solution, regardless of whether large or small displacements are specified. The iterations detect the contact status of the nodes. In the present study large sliding and large displacement applications are involved. Each contact pair has a pair-based depth which is obtained by averaging the depth of each contact element across all the contact elements.

2.2 Contact status

In the present study the contact of the steel bar and the concrete is taken as open on the initial stage. The contact can be closed only on some subareas of the contact zone due to the Poisson effect, affecting as a reduction of the rebar radius. The contact status, opened or closed, is monitored by the gap, calculated for the upper nodes as

$$g = z_2^c - z_2^s = \left[Z_2^c - u_2^c\right] - \left[Z_2^s - u_2^s\right], \tag{1}$$

where z_2^c and Z_2^c denote respectively the current and reference coordinate of a node from the concrete contact surface, z_2^s and Z_2^s denote respectively the current and the reference coordinates of a node from the steel contact surface, and u_2^c and u_2^s are the displacements of the concrete and the steel bar contact nodes, respectively, perpendicularly to the contact surface. The subscript 2 means the contact surface, described by the functions of the form of the steel bar elements.

The location of the contact detection points coincides with the location of the Gauss integration points. In alternation, the nodal point can be used.

2.3 Contact calculation method

In the basic Coulomb friction model, two contacting surfaces can carry shear stress up to a certain magnitude across their interface before they start to slide relative each other. This stage is known as *sticking* stage. The Coulomb friction model defines an equivalent shear stress $\bar{\tau}$ ($\bar{\tau} = \mu p + c$), at which sliding on the surface begins as a fraction of the contact pressure. Once the equivalent shear stress is exceeded, the two surfaces will slide relative to each other. This stage is known as *sliding* stage. The calculations determine when a point transition from sticking to sliding or vice versa. By default, Coulomb and shear stress friction are allowed as isotropic or orthotropic. The contact stiffness is assumed to be updated on each load step. In the models one extension of the classical Coulomb friction is used. The real constant $\bar{\tau}$ is the maximum contact friction with units of stress. This maximum contact friction stress can be introduced so that, regardless of the magnitude of normal contact pressure, sliding will occur if the friction stress reaches this value.

For surface-to-surface contacts five algorithms can be applied. Such algorithms are: Penalty method, Augmented Lagrangian method, Lagrange multiplier on contact normal and penalty on tangent, Pure Lagrange multiplier on contact normal and tangent and Internal multipoint constrained method. In the present study the Augmented Lagrangian method with gradient-base algorithm is used. This method can be interpreted as series of penalty methods, usually leads to better conditioning and is less sensitive to the magnitude of the contact stiffness. For Augmented Lagrangian method, normal and tangential contact stiffnesses are required. The penetration between the contact and the target

surfaces depends on normal stiffness. The Augmented Lagrangian method can be written symbolically in the form

$$\begin{bmatrix} k & -k \\ -k & k \end{bmatrix} \begin{Bmatrix} du_2^c \\ du_2^s \end{Bmatrix} = \begin{Bmatrix} -\lambda_k & -kg \\ \lambda & +kg \end{Bmatrix}, \tag{2}$$

or if the contact is non-sliding

$$\begin{bmatrix} k & -k \\ -k & k \end{bmatrix} \begin{Bmatrix} du_2^c \\ du_2^s \end{Bmatrix} = \begin{Bmatrix} -\lambda_k & -p \\ \lambda_k & +p \end{Bmatrix}. \tag{3}$$

In eqn. (2) k is a penalty parameter, λ_k is a Lagrange multiplier, identified here as "force" and $\lambda_{k+1} = \lambda_k + kg$. The components du_2^c and du_2^s give the ramp increment of the displacements. This method can be treated as compromise between the Penalty method and the Lagrange multiplier method. In the penalty approach the final gap must be non zero. On the other hand, for any Lagrange multiplier approach the equations are not positive defined and indeed have a zero diagonal for each multiplier term (Lagrange multiplier methods introduce zero diagonal terms in the stiffness matrix and any iterative solver will encounter a preconditioning matrix singularity with these methods). These computational difficulties are ignored in the concept of the Augmented Lagrangian method, the matrix $[k]$ is symmetric and positive defined.

2.4 Surface-to-surface contact

The surface-to-surface contact concept investigates the contact through the shape functions of the elements. After every iteration the value of τ stresses is checked and constitutes the states of the contact: if $\tau < \bar{\tau}$ then sticking stage is in being, or if $\tau > \bar{\tau}$, then sliding stage is observed.

This technique has some advantages in the case of different forms of the contact and target surfaces and anisotropic materials. To prevent rigid body motion the initial geometry must be checked and appropriate initial conditions must be defined. The adjustment of the initial contact conditions is important stage in the case of similar geometry and coordinates of the contact and target surfaces. In other words, the model must be built so that the contact pairs are in initial contact, i.e. open contact. The normal and tangential stiffness can be updated during the course of the analysis. In the computational models, presented in the paper, this option is used so that the stiffnesses to be automatically updated.

2.5 Concrete crack determination

The presence of a crack at an integration point is represented through modification of the stress-strain relations by introducing a plane of weakness in a

direction normal to the crack face. Also, a shear transfer coefficient β_t is introduced which represents a shear strength reduction factor for those subsequent loads which induce sliding across the crack face. If the cracks are developed in one direction only the stress-strain relation in based on the matrix

$$\left[D^{cr}\right]=\frac{E}{(1+\nu)}\begin{bmatrix} \frac{R^t(1+\nu)}{E} & 0 & 0 & 0 & 0 & 0 \\ 0 & \frac{1}{1-\nu} & \frac{\nu}{1-\nu} & 0 & 0 & 0 \\ 0 & \frac{\nu}{1-\nu} & \frac{1}{1-\nu} & 0 & 0 & 0 \\ 0 & 0 & 0 & \beta_t & 0 & 0 \\ 0 & 0 & 0 & 0 & \frac{1}{2} & 0 \\ 0 & 0 & 0 & 0 & 0 & \frac{\beta_t}{2} \end{bmatrix}. \quad (4)$$

In eqn. (4) the superscript *ck* signifies that the stress strain relations refer to a coordinate system parallel to principal stress directions. R^t is the slope, illustrated in fig.1,

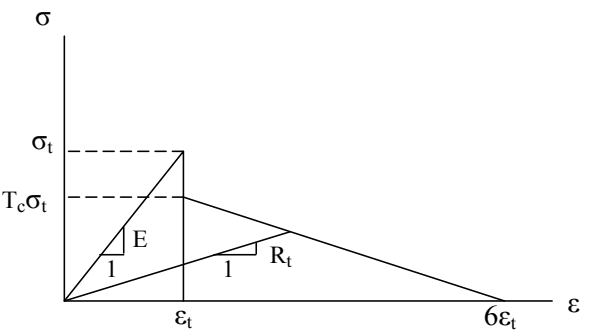

Figure 1: Strength of cracked condition.

where σ_t is uniaxial tensile cracking stress and T_c - multiplier for amount of tensile stress relaxation.

3 Generation of the computational model

The steel bar material model is assumed to be totally linear. It has good reasons for such an acceptation, because the ultimate normal stresses, obtained in the steel bar, are less than the yielding stress (yield point of the strain-stress curve) for the grade of the steel, used in the experiment.

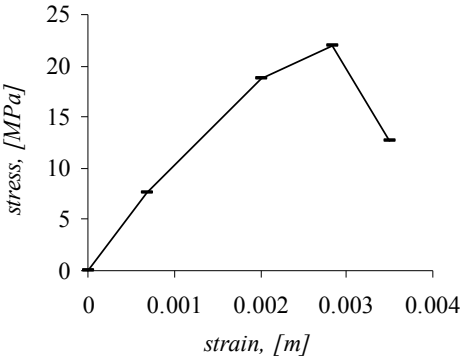

Figure 2: Assumed multi-linear strain-stress relation.

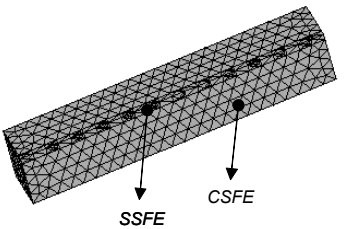

Figure 3: FEM model.

The coordinates of the characteristic points from the graph, fig. 2, shows the assumed multi-linear strain-stress relation for the concrete elements (CSFEs).

Geometrical characteristics correspond to experimental test entirely [12] and the boundary conditions applied to the model are constraining the displacements of the concrete nodes, the position of which is on the front area of the concrete solid. The load is transformed to a step-by-step displacement of the front area of the steel bar. The displacement of the reinforcement increases up to the moment of the contact failure. By reason of symmetry of the setting only quarter of the geometry is used. The discretization mesh is illustrated in fig. 3.

4 Numerical results and ductile capacity analysis

4.1 Numerical results

In the present research two models are generated. The first one, called Model A, is based on the multi-linear strain-stress relation, illustrated on fig.2. The bond-relative slip relation is juxtaposed with the relation, reported in [13], where the concrete material model is assumed as bi-linear. In addition, in the second model, called Model B, the aim of which is to simulate more adequately the concrete behaviour in a region close to the contact surface, a special option of the CSFEs is used. Such an option allows development of dispersed micro cracks in the volume of the concrete.

The value of ultimate force reported in [13] is $F_{pullout}^{sim} = 31.36\,kN$. The force, obtained by the experiment is $F_{pullout}^{\exp} = 22.12\,kN$. The relative difference between the two values is about 30%. In fig.4 can be seen the development of the bond stress-slip relation, in these two cases.

The ultimate forces during the extraction process obtained from Model A and Model B are respectively $F_{pullout}^{A} = 26.68\,kN$ and $F_{pullout}^{B} = 24.20\,kN$. Here, the relative differences in comparison with the test are 19% and 8%. The bond stress-slip relations concerning Model A and Model B are juxtaposed in fig.5.

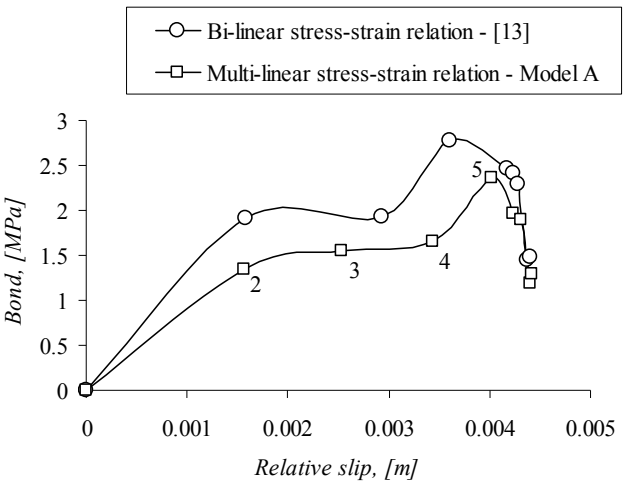

Figure 4: Bond-relative slip relations (Model, given in [13] vs. Model A).

There are two possible ways for the global failure to be achieved. The first way is the case where the tensile stresses exceed the tensile strength of the concrete. This failure mode can be called *splitting failure mode* and dominates in cases where the concrete is well penetrated in the isolated steel bar concavities. The mode like this is peculiar to deformed steel bars. Due to the Poisson effect the change of the steel bar radius leads to decreasing the normal contact stress between the bar and the concrete. In the case of a surrounding concrete, well-confining the isolated steel bar, the failure mode can be called *pullout failure mode*. Such failure mode is typical for plane bars.

The Model A can be classified as splitting failure model, similar to the model reported in [13], by reason of the softening, observed between the second and the third points, given on the relation bond stress-relative slip, see fig.4, and the following increase of the contact capacity. The global failure begins once the ultimate pullout force is reached. On this stage all the contact status of the pull-out process is sliding, despite of some local increase of the force, observed probably because of the specific non-smooth geometry of the contact.

4.2 Ductility capacity of the bond

The bond stress-slip relation, related to Model B, can be classified as ductile contact behaviour. This leads to the need to give a new meaning to the failure modes and pull-out process as a whole. The region of the curve, limited between the points (point 4 and point 6) determines the ductile capacity of the bond. The length of the section presents the ductile capacity of the mechanical bond.

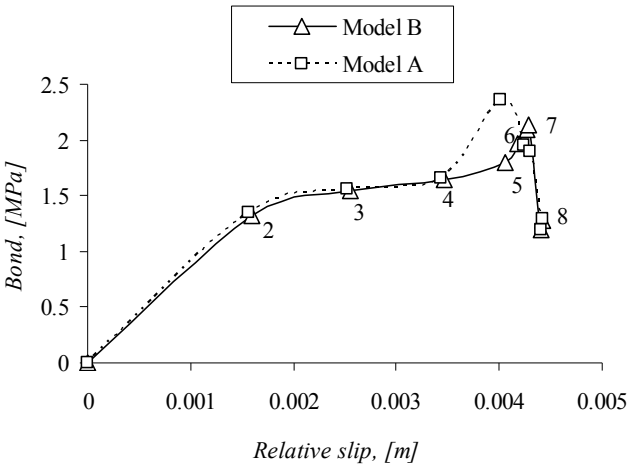

Figure 5: Bond-relative slip relations, (Model A vs. Model B).

5 Conclusions

It can be concluded, that the proposed in this paper FEM models adequately simulate the pull-out process of the isolated steel bar from the concrete body. The multi-linear idealization of the stress-strain relation, concerning the concrete, leads to ultimate force closer to the experiment. An additional reduction of the ultimate force is observed due to the dispersion micro crack option introduced to the near to the contact surface concrete elements. More realistic modelling of the non-linear behaviour of the concrete obviously leads to reduction of the value of the ultimate pull-out force.

The ductile capacity of the bond can be treated as an important part of the ductile capacity of the entire structure. The real ductile capacity of the bond is more than the capacity, obtained by proposed models, because the steel bar and the cured epoxy coating are assumed as a solid with material parameters equivalent to the steel as a material. This assumption underrates the real deformations, which have arisen in the mid-layer, and neglects the reciprocally displacements between the points on the steel surface and the points on surface of the epoxy coating. Despite of that, the thickness of the so-called mid-layer (the epoxy coating) is insignificant from geometrical point of view. In that layer can be accumulated additional energy of deformation and the length of the section between points (point 4 and point 6), see fig. 5, to be increased.

Acknowledgement

This paper has been supported by Grant Agency by European Social Fund, O.P "Human Resources Development", (No. BG051PO001/07/3.3.02.55/17.06.08).

References

[1] Gustafson P. David, Epoxy Update. *Concrete Reinforcing Steel Institute, Civ. Eng., ASCE,* **(58)10**, pp. 38-41, 1988.
[2] Choi, O. C., Hadje-Ghaffari, H. Darwin, D. & McCabe, S. L., Bond of epoxy-coated reinforcement: bar parameters. *ACI Materials Journal*, **88(2)**, pp. 207-217, 1991.
[3] Miller Gerald, K. Jennifer, and D. Darwin, Effect of Epoxy Coating Thickness on Bond Strength of Reinforcing Bars. *ACI Structural Journal*, **100(3)**, pp. 314-320, 2003.
[4] Cleary D. and J. Ramirez, Bond Strength of Epoxy-Coated Reinforcement. *ACI Materials Journal*, **88(2)**, pp. 146-149, 1991.
[5] Kayyali O. A. and S. R. Yeomans, Bond and slip of coated reinforcement in concrete. *Construction and Building Materials*, **9(4)**, pp. 219-226, 1995.
[6] Hamad S., Comparative Bond Strength of Coated and Uncoated Bars with Different Rib Geometry. *ACI Material Journal*, **92(6)**, pp. 579-590, 1995.
[7] Ldun E. and D. Darwin, Bond of Epoxy-Coated Reinforcement: Coefficient of Friction and Rib Face Angle. *ACI Structural Journal*, **96(4)**, pp. 609-615, 1999.
[8] Protasio F., Influence of Coatings on Bar-Concrete Bond. *Journal of Materials in Civ. Eng.*, **8(4)**, pp. 212-214, 1996.
[9] Cairns J. and R. Abdullah, Fundamental Test on the Effect of an Epoxy Coating on Bond Strength. *ACI Materials Journal*, **91(4)**, pp. 331-338, 1994.
[10] Cusens, A. R., Z. Yu, Pullout Tests of Epoxy-Coated Reinforcement in Concrete. *Cement & Concrete Composites*, Vol.**14**, pp. 269-276, 1992.
[11] Mo Y., and J. Chan, Bond and Slip of Plain Rebars in Concrete, *Journal of Materials in Civil Engineering*, **8(4)**, pp. 208-211, 1996.
[12] Yanakieva A., Bonding between protected steel reinforcement and concrete, *Proc. of the IX National Congress on Theoretical and Applied Mechanics*: Varna, Bulgaria, pp.627-632, 2001.
[13] Yanakieva A. & Kazakov K., FEM numerical simulation of bond-slip behaviour between epoxy coated plain steel bars and concrete, *Proc. of the Int. Conf. Of FCE STU*, Bratislava, Slovakia, 2008.
[14] Kazakov K., *The finite element method for structural modelling*: VSU publishing house, Sofia, 2006.